

Probe absorption by an atom in a strong finite-linewidth laser field

Henk F. Arnoldus and Thomas F. George

*Departments of Physics & Astronomy and Chemistry, 239 Fronczak Hall,
State University of New York at Buffalo, Buffalo, New York 14260*

(Received 18 July 1986)

The probe-absorption spectrum of an atom, immersed in a finite-bandwidth laser field and a perturber gas, is calculated. Both single-mode and multimode excitation is treated, and the solutions of the occurring stochastic multiplicative processes are obtained in closed form. Different features of the profile are discussed, and it is seen that the spectrum is not determined by the laser line shape only, but that knowledge of the higher-order stochastic properties of the driving field is required.

I. INTRODUCTION

The interaction of a two-level atom with an intense monochromatic laser field is well understood.¹⁻³ The coherent excitation of the system amounts to Rabi oscillations of the level populations,⁴ and spontaneous decay provides the relaxation mechanism for the evolution to a unique steady state. Decay of the excited state is accompanied by the emission of a fluorescent photon, which can be observed with a photomultiplier tube. The spectral distribution of the fluorescence radiation is the Fourier-Laplace transform of the time regression of the atomic-dipole correlation function, which is determined by the time evolution of the atomic density operator. Hence the details of the interaction of the atom with the strong radiation field are reflected in the spectrum of the spontaneously emitted radiation. The generic method of studying the interaction of an atom with a radiation field is by the spectrally resolved detection of its emitted fluorescence, and consequently the theory has focused on the details of atomic emission line shapes. A two-level system in a strong driving field exhibits a three-line spectrum, which can be understood in a dressed-state picture,⁵ and has been observed in experiment.^{6,7}

An alternative method for probing the laser-atom interaction is by scanning a weak laser over the atomic resonance, and measuring the absorption of the joint system of the atom and strong driving field. The probe-absorption profile is germane to the spontaneous-emission profile in that it is also determined by the atomic-dipole correlation function. This implies that the fluorescence and absorption spectrum essentially contain similar information. However, the net absorption is a balance between stimulated absorption and emission, which causes the cancellation of the line corresponding to the Rayleigh line at the optical frequency in the fluorescence triplet. Hence the absorption profile is intrinsically a two-line spectrum,⁸ which can again be understood from the dressed-state picture.⁹ Furthermore, the absorption can assume negative values, which implies the domination of stimulated emission in the probe beam over the absorption. This peculiar feature can only appear in the presence of the driving

laser, which supplies the energy for the amplification, as shown by Mollow.⁸ The different properties of the absorption line shapes have been verified experimentally by Wu *et al.*¹⁰

An atom in a laser field will, in general, be subject to dephasing mechanisms, which affect the absorption profile. In vapor experiments the atoms are immersed in a buffer gas. The most pronounced modification is then brought about by collisions with neutral atoms, which broadens the absorption line.¹¹ Another inevitable randomization of the atomic dipole results from the laser linewidth. The fluctuating laser phase broadens the laser line, and its effect on the absorption profile was studied by Agarwal for a Gaussian diffusive phase.¹² Collisional redistribution of radiation and laser-bandwidth-induced energy transfer between spectral lines alter atomic spectra in a similar, but not identical way.¹³

For a weak driving laser, which is in close resonance with the atomic transition frequency, the collisional perturbations are fairly well accounted for by an impact-limit approach,¹⁴ and the laser-linewidth modifications are completely determined by the spectral profile of the laser. In the situation of high irradiance, or with a large detuning, the spectra exhibit distinct lines. If we denote the line separation by $|\Omega'|$, then $|\Omega'|$ is a characteristic frequency of the atom in the strong driving field (dressed atom), and its inverse $|\Omega'|^{-1}$ is not necessarily large in comparison with the time duration of a collision and with the laser coherence time. Then both the impact limit and the phase-diffusion model cannot be expected anymore to account for the details of the line shapes. Extensions beyond the impact limit of line broadening have been developed (binary-collision approximation,¹⁵ Fano projection technique¹⁶), and a finite laser coherence time was incorporated by the assumption that the laser phase obeys Ornstein-Uhlenbeck statistics.¹⁷⁻²⁰ These theories have been applied mainly to the problem of fluorescence.

In this paper we consider the laser-linewidth effects for both single-mode and multimode excitation on the atomic absorption profile. Since the emphasis is on the bandwidth-induced modifications, we include collisions only in the impact limit. This will still enable us to keep

track of collisional intensity transfer, but without every detail which arises due to the dynamics of a specific collision.

II. LASER MODELS

Since the atomic response to the strong radiation field is not determined by just the spectral distribution of the laser, we have to specify the details of the model. First, we outline the general concepts, and then we specify the models which are treated in this paper. The electric component of the field at the position of the atom is represented by

$$\mathbf{E}(t) = E_0 \text{Re} \epsilon_L e^{-i[\omega_L t + \phi(t)]}. \quad (2.1)$$

Here, E_0 is the real amplitude, ϵ_L is the unit polarization vector ($\epsilon_L \cdot \epsilon_L^* = 1$), ω_L is the optical frequency, and the phase $\phi(t)$ is taken to be a real-valued stochastic process. The distinct models arise by adopting different stochastic properties of $\phi(t)$. The steady-state spectral profile of the field equals²¹

$$I_L(\omega) = \lim_{t \rightarrow \infty} \frac{1}{\pi} \text{Re} \int_0^\infty d\tau e^{i(\omega - \omega_L)\tau} \langle e^{-i[\phi(t+\tau) - \phi(t)]} \rangle_{\text{st}}, \quad (2.2)$$

where the notation $\langle \dots \rangle_{\text{st}}$ indicates an average over the stochastics of the phase (the angular brackets $\langle \dots \rangle$ will be reserved for a quantum average). For a time-independent phase the profile reduces to $I_L(\omega) = \delta(\omega - \omega_L)$, but fluctuations in $\phi(t)$ will broaden this line around the central frequency ω_L . The limit $t \rightarrow \infty$ in Eq. (2.2) eliminates possible switch-on effects, and it is, of course, assumed that the stationary state exists for a given process $\phi(t)$. Integration of $I_L(\omega)$ over its spectral width gives

$$\int d\omega I_L(\omega) = 1, \quad (2.3)$$

which shows that the fluctuating phase redistributes the power over a frequency range around ω_L , but without affecting the overall strength of the field.

It might appear that any choice of $\phi(t)$ yields a single laser line around ω_L . Such is, however, not the case. We can write Eq. (2.2) alternatively as

$$I_L(\omega) = \frac{1}{\pi} \text{Re} \int_0^\infty d\tau e^{i\omega\tau} \left\langle \exp \left[-i \int_0^\tau [\omega_L + x(s)] ds \right] \right\rangle_{\text{st}}, \quad (2.4)$$

with $x(t) = \dot{\phi}(t)$, and then consider the properties of the time derivative $x(t)$ of the phase to be given. Obviously, the process $x(t)$ must be stationary in order to guarantee the time independence of the profile. Hence we can omit the limit $t \rightarrow \infty$ in this representation, and the probability distribution $P(x)$ of $x(t)$ must be independent of time. The structure of the profile becomes quite transparent if we consider the static limit of the process $x(t)$, where $x(t)$ is independent of time for every realization of the process.^{22,23} Then the average in Eq. (2.4) is a single-time average, which is easily found to be

$$I_L(\omega) = P(\omega - \omega_L). \quad (2.5)$$

This reveals that the laser profile is identical to the probability distribution of $x(t)$ in this case, which implies that the possible values of $\omega_L + x(t)$ can be considered as the laser modes. From Eq. (2.4) it can also be inferred that $\omega_L + x(t)$ can be regarded as the instantaneous laser frequency. For a nonstatic process $x(t)$, the field will switch between the occurring values of $x(t)$, and thereby distort the profile (2.5). If we allow $P(x)$ to consist of a sum of δ functions, then the profile $I_L(\omega)$ represents a genuine multimode field. Hence our model (2.1) of the finite-linewidth laser field pertains to both single-mode and multimode radiation, and can therefore be regarded as a quite general representation of a laser field, although other models could be conceived.²⁴

The theory of laser-linewidth effects on the atomic response to strong incident radiation is essentially a topic in stochastic processes. With recent developments in the theory of stochastic differential equations, it has become feasible to average two-time operator-valued quantities explicitly, and without any approximation (decorrelation assumptions). The most simple example is the laser profile itself. Let us introduce the stochastic function

$$g(t', t) = \exp \left[-i \int_t^{t'} ds x(s) \right], \quad (2.6)$$

which obeys the equation

$$i \frac{d}{dt'} g(t', t) = x(t') g(t', t) \quad (2.7)$$

and the initial condition

$$g(t, t) = 1. \quad (2.8)$$

With the Fourier-Laplace transform of its average,

$$\tilde{g}(\omega, t) = \int_t^\infty dt' e^{i\omega(t'-t)} \langle g(t', t) \rangle_{\text{st}} \quad (2.9)$$

the laser profile can be written as

$$I_L(\omega) = \lim_{t \rightarrow \infty} \frac{1}{\pi} \text{Re} \tilde{g}(\omega - \omega_L, t). \quad (2.10)$$

This implies that if we are able to solve the multiplicative stochastic differential equation (2.7) for the average $\langle g(t', t) \rangle_{\text{st}}$, then we can obtain the laser profile after a Fourier-Laplace transform.

The class of single-mode models we consider assumes the phase $\phi(t)$ to be a homogeneous Markov process,²⁵ defined on $-\infty < \phi(t) < \infty$, and with a transition rate from ϕ to ϕ' which depends only on the phase difference $\phi - \phi'$. This process is usually called the independent-increment process,²⁶ and it has the transition rate $w(\phi - \phi')$ as an arbitrary parameter function. We suppose that $w(\phi) = w(-\phi)$, which implies that the phase fluctuations broaden the laser line, without shifting it. The probability distribution $P(\phi, t)$ for the phase $\phi(t)$ is given by the Fourier integral

$$P(\phi, t) = \frac{1}{2\pi} \int_{-\infty}^\infty d\rho \exp \left[-i\rho\phi - t \int_{-\infty}^\infty d\eta (1 - e^{i\rho\eta}) w(\eta) \right] \quad (2.11)$$

in terms of the prescribed function $w(\eta)$. The conditional probability for the occurrence of $\phi(t+\tau)=\phi_2$, if $\phi(t)=\phi_1$, follows from the relation

$$P_\tau(\phi_2|\phi_1)=P(\phi_2-\phi_1, \tau), \quad \tau \geq 0. \quad (2.12)$$

Together with Eq. (2.11) and the Markov property of the probability distributions, this relation fixes the stochastic properties of the phase. Notice the appearance of t in the integrand of Eq. (2.11), which shows that $\phi(t)$ is nonstationary. It is a non-Gaussian diffusion process, in general.

The multiplicative stochastic differential equations for this phase model have been solved in a previous paper,¹³ and the solutions were applied to evaluate the fluorescence spectrum of a two-level atom in a perturber bath. It turned out that only two parameters of the process determine the atomic line shapes, rather than the very details of $w(\eta)$. They are

$$\lambda = \int_{-\infty}^{\infty} d\eta (1 - \cos\eta) w(\eta), \quad (2.13)$$

$$\lambda' = \int_{-\infty}^{\infty} d\eta [1 - \cos(2\eta)] w(\eta), \quad (2.14)$$

which are both real, and obey the inequality

$$0 \leq \lambda' \leq 4\lambda. \quad (2.15)$$

Any function $w(\eta)$ gives rise to the laser profile

$$I_L(\omega) = \frac{\lambda/\pi}{(\omega - \omega_L)^2 + \lambda^2}, \quad (2.16)$$

which is a Lorentzian with half width at half maximum (HWHM) equal to λ . Hence the parameter λ has the clear interpretation of the laser linewidth, and it can be shown that λ' depends on the higher-order photon correlations of the laser field. This means that any appearance of λ' in an atomic spectrum indicates that knowledge of the laser profile is not sufficient to evaluate the atomic response to the laser.

In the Gaussian limit of this independent-increment process, which is the common phase-diffusion or Wiener-Lévy process, the parameter λ' is no longer independent but is related to λ as $\lambda' = 4\lambda$. A different single-mode laser model can be defined by considering the phase as a stationary random-jump process.^{27,28} This is known as the Lorentz wave.^{29,30} However, it can be shown³¹ that this model yields identical results as the independent-increment process in the limit $\lambda' \rightarrow \lambda$. Therefore, our single-mode laser model covers the more familiar models as special cases ($\lambda' = \lambda$ and $\lambda' = 4\lambda$), but is more general, since we have only the restriction (2.15).

For a multimode laser we prescribe the stochastics of $x(t)$. The process $x(t)$ is assumed to be a stationary Markov process with probability distribution $P(x)$ and conditional probability

$$P_\tau(x_2|x_1) = e^{-\gamma\tau} \delta(x_2 - x_1) + P(x_2)(1 - e^{-\gamma\tau}), \quad \tau \geq 0, \quad (2.17)$$

where $\gamma \geq 0$ is the switching rate between the modes, or the inverse laser coherence time. Consider a discrete distribution $P(x)$. Then for $\gamma \rightarrow 0$ the laser profile is given by Eq. (2.5), which is a sum of δ functions in this case. However, a finite γ^{-1} can be interpreted as the average

“dwelling time” in a single mode, and hence the switching between different modes causes a broadening of every line.³² For the process $x(t)$, which is generally referred to as the random-jump process, we can solve the stochastic differential equation (2.7), and the Fourier-Laplace transform of the solution reads³³

$$I_L(\omega) = \frac{1}{\pi} \operatorname{Re} \frac{1}{1 - \gamma \int dx P(x) \frac{i}{\omega - \omega_L - x + i\gamma}} \times \int dx P(x) \frac{i}{\omega - \omega_L - x + i\gamma}. \quad (2.18)$$

In the case where $P(x)$ is a sum of δ functions, the integrals reduce to summations. Figure 1 illustrates the dependence of this profile on the switching rate γ for a three-mode laser.

The nomenclature single-mode and multimode field pertains to prescribed stochastics of $\phi(t)$ and $x(t)$, respectively, but a single-peak distribution $P(x)$, centered around $x=0$, actually represents a single laser line around $\omega = \omega_L$. We pointed out in a previous paper, Ref. 33, that the choice of a Gaussian $P(x)$ greatly resembles the commonly applied single-mode model with a finite coherence time,¹⁷⁻²⁰ where $x(t)$ is taken to be the Ornstein-Uhlenbeck process. It gives rise to all the desired features of a realistic laser model, e.g., Poissonian photon statistics, a Lorentzian profile near the line center, and Gaussian in the line wings. The so-called cutoff frequency in the Ornstein-Uhlenbeck process, which determines the transition from a Lorentzian to a Gaussian with increasing ω , equals γ in our multimode model. Furthermore, the mode-correlation function $\langle x(t)x(t') \rangle_{st}$ decays exponentially in both models. Hence our unified “multimode” theory incorporates the standard single-mode model as a special case.

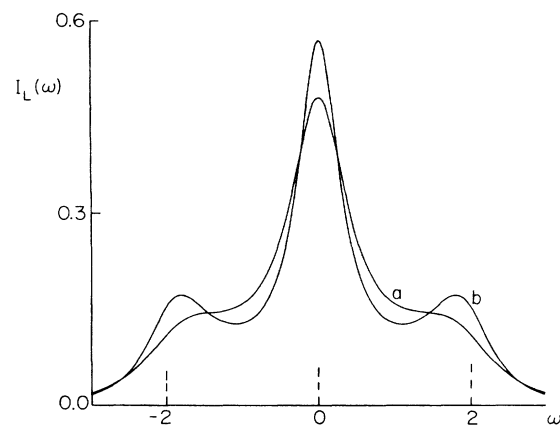


FIG. 1. Plot of the laser profile $I_L(\omega)$ from Eq. (2.18), shifted over ω_L , for the case of a three-mode field. The dotted lines indicate the positions of the modes, which have a relative probability distribution of 1:2:1. Curve *a* (*b*) corresponds to $\gamma = 1$ (0.7). All frequencies are in the same, arbitrary, units.

III. EQUATION OF MOTION

The two-level atom in a perturber bath, subject to spontaneous decay and immersed in a strong laser field, obeys the equation of motion

$$i\hbar \frac{d\rho}{dt} = [H_a + H_{ar}(t), \rho] - i\hbar \Gamma \rho - i\hbar \Phi \rho, \quad \rho^\dagger = \rho, \quad \text{Tr} \rho = 1. \quad (3.1)$$

In terms of the projectors $P_e = |e\rangle\langle e|$ and $P_g = |g\rangle\langle g|$ onto the excited state $|e\rangle$ and the ground state $|g\rangle$, respectively, the atomic Hamiltonian can be represented as

$$H_a = \hbar\omega_e P_e + \hbar\omega_g P_g, \quad (3.2)$$

and the coupling of the field (2.1) with the atomic dipole μ attains the form

$$H_{ar}(t) = -\frac{1}{2} \hbar \Omega e^{-i[\omega_L t + \phi(t)]} d + \text{H.c.} \quad (3.3)$$

in the rotating-wave approximation. Here we have denoted the coupling strength by $\Omega = E_0 | \langle e | \mu \cdot \epsilon_L | g \rangle | / \hbar$ (Rabi frequency), and adopted the notation $d = |e\rangle\langle g|$ for the atomic raising operator. It is convenient to introduce a Liouville operator L_g , which is defined by its action on a Hilbert space operator ρ , according to

$$L_g \rho = [P_g, \rho]. \quad (3.4)$$

Then the spontaneous-decay operator Γ can be written as³⁴

$$\Gamma \rho = \frac{1}{2} A L_g^2 \rho + A (P_e - P_g) \langle e | \rho | e \rangle \quad (3.5)$$

in terms of the Einstein coefficient A for spontaneous decay of the two-level system. The collisional relaxation is incorporated in the operator Φ , defined by

$$\Phi \rho = (\alpha L_g^2 - i\beta L_g) \rho, \quad (3.6)$$

which contains the collisional width α and shift β of the low-intensity absorption profile. The quantities α and β can be expressed in elements of the S matrix for a single collision, averaged over the perturber velocity distribution.³⁵

The equation of motion (3.1) is a stochastic differential equation, due to the appearance of $\phi(t)$ in $H_{ar}(t)$, and hence $\rho(t)$ is a stochastic process. Evaluation of the average over the phase fluctuations is greatly facilitated by a stochastic transformation of $\rho(t)$,³⁶⁻³⁸ which eliminates the fast oscillations with the optical frequency ω_L in the Hamiltonian, and turns the equation of motion (3.1) into a standard form from the point of view of stochastic processes. This transformation can be written transparently in terms of the operator L_g from Eq. (3.4). We define $\sigma(t)$ by

$$\sigma(t) = e^{-i[\omega_L t + \phi(t)] L_g} \rho(t). \quad (3.7)$$

From Eq. (3.1) we then obtain the equation of motion

$$i\hbar \frac{d\sigma}{dt} = [\hbar[\omega_L + x(t)] P_g + H_a + H_{ar}(0), \sigma] - i\hbar \Gamma \sigma - i\hbar \Phi \sigma, \quad (3.8)$$

which now contains $x(t)$ as the driving stochastic process, rather than the phase $\phi(t)$ itself. Then the dressed-atom Hamiltonian is defined by

$$H_d = -\frac{1}{2} \hbar [\Delta (P_e - P_g) + \Omega (d + d^\dagger)], \quad (3.9)$$

where $\Delta = \omega_L - (\omega_e - \omega_g)$ is the detuning of the laser from resonance. With the abbreviation for the corresponding Liouvillian

$$L_d(\omega_L) \rho = \hbar^{-1} [H_d, \rho], \quad (3.10)$$

where the ω_L dependence is displayed explicitly for later purposes, the equation of motion for $\sigma(t)$ acquires the simple form

$$i \frac{d\sigma}{dt} = [L_d(\omega_L) + x(t) L_g - i\Gamma - i\Phi] \sigma, \quad \sigma^\dagger = \sigma, \quad \text{Tr} \sigma = 1. \quad (3.11)$$

Notice that this equation is equivalent to Eq. (3.1) since the transformation (3.7) can be inverted.

IV. POPULATIONS

After an expansion of the exponential in the transformation (3.7), we can relate the matrix elements of $\rho(t)$ and $\sigma(t)$. In particular, we find

$$\langle e | \sigma(t) | e \rangle = \langle e | \rho(t) | e \rangle, \quad (4.1)$$

and from $\text{Tr} \rho(t) = \text{Tr} \sigma(t) = 1$ it follows that also the populations of the ground state of $\sigma(t)$ and $\rho(t)$ are equal. The transformation only affects the coherences. Hence the stochastic average of the populations of the levels can be found from $\langle \sigma(t) \rangle_{\text{st}}$. Due to spontaneous decay, collisions, and the laser linewidth, the solution $\langle \sigma(t) \rangle_{\text{st}}$ will reach the steady state

$$\bar{\sigma} = \lim_{t \rightarrow \infty} \langle \sigma(t) \rangle_{\text{st}}, \quad (4.2)$$

but the solution $\sigma(t)$ of Eq. (3.11) will never evolve to a time-independent value, because of the persisting fluctuations in $x(t)$. Of particular interest are the steady-state populations

$$n_e = \langle e | \bar{\sigma} | e \rangle, \quad n_g = \langle g | \bar{\sigma} | g \rangle = 1 - n_e. \quad (4.3)$$

For the processes $x(t)$ under consideration, it will turn out that the stochastic averages can be expressed more easily in the Fourier-Laplace domain. Therefore we adopt the transformation

$$\tilde{\sigma}(\omega) = \int_{t_0}^{\infty} dt e^{i\omega(t-t_0)} \langle \sigma(t) \rangle_{\text{st}}, \quad (4.4)$$

which amounts to the identity

$$\bar{\sigma} = \lim_{\omega \rightarrow 0} -i\omega \tilde{\sigma}(\omega) \quad (4.5)$$

for the steady-state density matrix.

Suppose that a nonstochastic initial state $\sigma(t_0)$ is given. For a single-mode laser (independent-increment process) the average atomic state is then found to be¹³

$$\tilde{\sigma}(\omega) = \frac{i}{\omega - L_d(\omega_L) + iW_0 + i\Gamma + i\Phi} \sigma(t_0) \quad (4.6)$$

in terms of an operator inversion. The laser linewidth appears to be accounted for by the effective relaxation operator

$$W_0 = \lambda L_g^2, \quad (4.7)$$

which is proportional to and depends only on the linewidth λ . Hence the details of the laser-field stochastics do not enter the solution for the average density operator. The unique steady state follows from

$$[L_d(\omega_L) - iW_0 - i\Gamma - i\Phi]\bar{\sigma} = 0, \quad \bar{\sigma}^\dagger = \bar{\sigma}, \quad \text{Tr}\bar{\sigma} = 1, \quad (4.8)$$

which can be solved immediately. The population of the excited state becomes

$$n_e = \frac{\frac{1}{2}\Omega^2(\frac{1}{2}A + \lambda + \alpha)}{\Omega^2(\frac{1}{2}A + \lambda + \alpha) + A[(\Delta - \beta)^2 + (\frac{1}{2}A + \lambda + \alpha)^2]}, \quad (4.9)$$

and the coherence of $\bar{\sigma}$ is found to be

$$\langle e | \bar{\sigma} | g \rangle = \frac{iA[\frac{1}{2}A + \lambda + \alpha + i(\Delta - \beta)]}{\Omega(\frac{1}{2}A + \lambda + \alpha)} n_e. \quad (4.10)$$

This determines explicitly $\bar{\sigma}$ for a single-mode driving field.

Combination of the definition (3.9) of H_d with the fact that $P_e + P_g$ equals the unit operator for a two-level atom enables us to write

$$L_d(\omega_L) + x(t)L_g = L_d(\omega_L + x(t)). \quad (4.11)$$

With this observation, the equation of motion (3.11) can be cast in the form

$$i\frac{d\sigma}{dt} = [L_d(\omega_L + x(t)) - i\Gamma - i\Phi]\sigma. \quad (4.12)$$

Then, the stochastic average $\bar{\sigma}(\omega)$ for the random-jump process (multimode field) can be expressed in the resolvent³⁹⁻⁴¹

$$U(\omega_1, \omega_2) = \frac{i}{\omega_1 + i\gamma - L_d(\omega_L + \omega_2) + i\Gamma + i\Phi}, \quad (4.13)$$

provided that the initial value $\sigma(t_0)$ is not stochastic (e.g., prescribed). The equivalent of Eq. (4.6) now becomes

$$\bar{\sigma}(\omega) = \frac{1}{1 - \gamma} \int dx P(x) U(\omega, x) \sigma(t_0), \quad (4.14)$$

and the steady-state density operator is the solution of

$$\int dx P(x) [1 - \gamma U(0, x)] \bar{\sigma} = 0, \quad (4.15)$$

where we used $\int dx P(x) = 1$. The operator $U(0, x)$ is the inverse of an x -dependent 4×4 matrix, and the feasibility of an analytic integration depends on the form of $P(x)$. For a discrete distribution the integral reduces to a simple summation, and Eq. (4.15) can be solved directly for $\bar{\sigma}$. In Fig. 2 the behavior of the steady-state population n_e as a function of the mode-switching rate γ is plotted for the three-mode laser from Fig. 1.

In the limit $\gamma \rightarrow \infty$, which implies a very fast mode

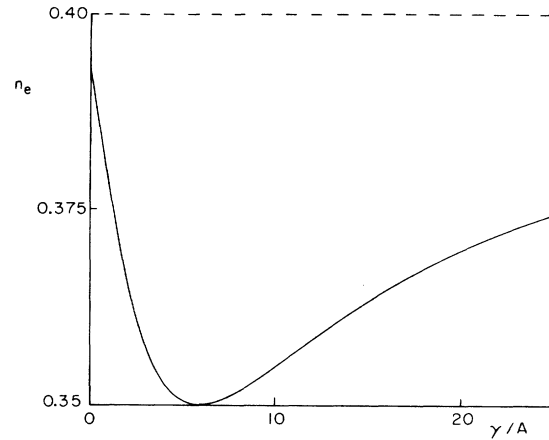


FIG. 2. The excited-state population n_e for the case of a three-mode laser field, calculated from Eq. (4.15), as a function of the switching rate γ . Frequencies are in the unit of the Einstein coefficient A . The laser modes are situated at $\omega_L - 2A$, ω_L , and $\omega_L + 2A$, with probability distributions of 0.25, 0.5, and 0.25, respectively. The Rabi frequency equals $\Omega = 5A$, and the detuning from resonance is $\Delta - \beta = 3A$ ($\omega_L = \omega_0 + \beta + 3A$). The collisional width is $\alpha = 1.5A$. For $\gamma \rightarrow \infty$ the population approaches the asymptotic value $n_e = 25/63$, which is indicated by the dotted line.

switching, the atomic system responds only to the average $\langle x(t) \rangle_{st}$.⁴² For a symmetric profile, like the three-mode laser, we have $\langle x(t) \rangle_{st} = 0$, and hence the results reduce to the situation of monochromatic irradiation. In particular, the population of the excited level becomes Eq. (4.9) with $\lambda = 0$, which is the dotted line in Fig. 2.

V. ABSORPTION PROFILE

A weak probe laser, with power I_p (energy flow per unit of time through a unit area, perpendicular to the direction of propagation), frequency ω , and polarization ϵ_p , is tuned over the atomic resonance. The atomic dipole μ absorbs photons from and emits photons in the beam. A formal expression for the absorption profile reads⁴³

$$I_A(\omega) = BI_p \lim_{t \rightarrow \infty} \frac{1}{\pi} \text{Re} \int_0^\infty d\tau e^{i\omega\tau} \times \langle \text{Tr} \rho(t) [d^\dagger(t + \tau), d(t)] \rangle_{st}, \quad (5.1)$$

which is the number of absorbed photons per unit of time. The two terms in the commutator pertain to stimulated absorption and emission, and the spectrum equals the balance between these two processes. Stimulated transitions are governed by the Einstein B coefficient,

$$B = \frac{\pi}{\epsilon_0 \hbar^2 c} |\langle e | \mu \cdot \epsilon_p | g \rangle|^2, \quad (5.2)$$

which appears only as an overall factor.

In order to evaluate the absorption spectrum, we have

to find the dipole correlation $\langle \cdots \rangle_{\text{st}}$ from Eq. (5.1). If we denote the atomic evolution operator by $X(t, t')$, we can write

$$\rho(t) = X(t, t')\rho(t'), \quad (5.3)$$

and the form of $X(t, t')$ follows after integration of the equation of motion (3.1). Subsequently, we transform the Heisenberg representation from Eq. (5.1) to the Schrödinger representation, which yields the relation

$$\begin{aligned} \langle [d^\dagger(t'), d(t)] \rangle &= \text{Tr} \rho(t) [d^\dagger(t'), d(t)] \\ &= \text{Tr} d^\dagger X(t', t) [d, \rho(t)], \end{aligned} \quad (5.4)$$

for $t' \geq t$. With Eq. (3.7) we then obtain the equivalent σ -picture representation,

$$\begin{aligned} \langle [d^\dagger(t'), d(t)] \rangle &= e^{-i[\omega_L(t'-t) + \phi(t') - \phi(t)]} \\ &\times \text{Tr} d^\dagger Y(t', t) [d, \sigma(t)], \quad t' \geq t \end{aligned} \quad (5.5)$$

where $Y(t', t)$ is the evolution operator for $\sigma(t')$, as it is determined by Eq. (3.11). This dipole correlation function can be written as

$$\langle [d^\dagger(t'), d(t)] \rangle = e^{-i\omega_L(t'-t)} \text{Tr} d^\dagger C(t', t), \quad (5.6)$$

where the two-time stochastic operator $C(t', t)$ is defined by

$$C(t', t) = e^{-i[\phi(t') - \phi(t)]} Y(t', t) [d, \sigma(t)]. \quad (5.7)$$

Differentiating this expression with respect to t' , and recalling that $Y(t', t)$ is the evolution operator for $\sigma(t')$, we obtain the equation of motion for $C(t', t)$ for $t' \geq t$,

$$i \frac{d}{dt'} C(t', t) = [L_d(\omega_L) + x(t')(L_g + 1) - i\Gamma - i\Phi] C(t', t), \quad (5.8)$$

where the initial condition reads

$$C(t, t) = [d, \sigma(t)]. \quad (5.9)$$

Notice that the regression equation (5.8) is not identical to the evolution equation (3.11) for the atomic density operator $\sigma(t)$, in that L_g has been replaced by $L_g + 1$. This is due to the exponential in Eq. (5.7). If we can solve Eq.

$$I_A(\omega) = BI_p \frac{1}{\pi} \text{Re} \text{Tr} d^\dagger \frac{i}{\omega - \omega_L - L_d(\omega_L) + iW_+ + i\Gamma + i\Phi} [d, \bar{\sigma}] \quad (6.3)$$

for the absorption profile. Comparison of W_+ with the operator $W_0 = \lambda L_g^2$, which governs the laser-linewidth modifications on the time evolution of the atomic density matrix, shows that the time regression of the atomic dipole is affected in quite a different way. In particular, W_+ involves the second laser parameter λ' , and hence the absorption profile is not determined by the laser line shape alone.

With some matrix algebra we can evaluate expression (6.3) explicitly in terms of the elementary parameters. We obtain

$$\begin{aligned} I_A(\omega) &= BI_p (n_g - n_e) \frac{1}{\pi} \text{Re} \left\{ \Omega^2 \left(\frac{1}{2} A + \frac{1}{2} \lambda' + \alpha - i\Lambda \right) \right. \\ &\quad + (A + \lambda - i\Lambda) \left[\frac{1}{2} A + \lambda' + \alpha + i(\Delta - \beta - i\Lambda) \right] \left[\frac{1}{2} A + \alpha - i(\Delta - \beta + i\Lambda) \right] \}^{-1} \\ &\quad \times \left[\frac{1}{2} \Omega^2 + (A + \lambda - i\Lambda) \left[\frac{1}{2} A + \lambda' + \alpha + i(\Delta - \beta - i\Lambda) \right] \right. \\ &\quad \left. - \frac{\frac{1}{2} \Omega^2}{(\Delta - \beta)^2 + (\frac{1}{2} A + \lambda + \alpha)^2} \left[\frac{1}{2} A + \lambda + \alpha - i(\Delta - \beta) \right] \left[\frac{1}{2} A + \lambda' + \alpha + i(\Delta - \beta - i\Lambda) \right] \right] \right\}, \end{aligned} \quad (6.4)$$

(5.8) for the stochastic average $\langle C(t', t) \rangle_{\text{st}}$, and then take its Fourier-Laplace transform

$$\tilde{C}(\omega, t) = \int_t^\infty dt' e^{i\omega(t'-t)} \langle C(t', t) \rangle_{\text{st}}, \quad (5.10)$$

we can express the absorption profile in this solution as

$$I_A(\omega) = BI_p \lim_{t \rightarrow \infty} \frac{1}{\pi} \text{Re} \text{Tr} d^\dagger \tilde{C}(\omega - \omega_L, t). \quad (5.11)$$

Comparison with Sec. II shows the close resemblance with the evaluation of the laser profile. We merely replace $g(t', t)$ by $C(t', t)$. The important differences are that (1) the quantity $C(t', t)$ is operator valued, and (2) the initial condition of $C(t', t)$, Eq. (5.9), is a stochastic operator as a function of time, whereas $g(t, t) = 1$.

The integrated profile follows from Eqs. (5.10) and (5.11). For any laser spectrum we find

$$\int d\omega I_A(\omega) = BI_p \langle C(t, t) \rangle_{\text{st}}, \quad (5.12)$$

which is again

$$\int d\omega I_A(\omega) = BI_p \text{Tr} d^\dagger [d, \sigma] = BI_p (n_g - n_e) \geq 0. \quad (5.13)$$

Therefore the integrated spectrum is completely determined by the steady-state density matrix $\bar{\sigma}$, which was evaluated in the previous section.

VI. SINGLE MODE

The stochastic differential equation (5.8) is easily solved for its average $\langle C(t', t) \rangle_{\text{st}}$ in the case that the phase $\phi(t)$ is the independent-increment process.¹³ The result is

$$\langle C(t', t) \rangle_{\text{st}} = e^{-i[L_d(\omega_L) - iW_+ - i\Gamma - i\Phi](t'-t)} \langle C(t, t) \rangle_{\text{st}}, \quad (6.1)$$

where the operator W_+ , which accounts for the laser linewidth, takes the form

$$W_+ \rho = \lambda(P_e \rho P_e + P_g \rho P_g) + \lambda' P_g \rho P_e. \quad (6.2)$$

Next we take the Fourier-Laplace transform, use Eq. (5.9), and take the limit $t \rightarrow \infty$. We then obtain the expression

with $\Lambda = \omega - \omega_L$. The integrated profile equals $BI_p(n_g - n_e)$, and from Eq. (4.9) we find

$$n_g - n_e = \frac{A[(\Delta - \beta)^2 + (\frac{1}{2}A + \lambda + \alpha)^2]}{\Omega^2(\frac{1}{2}A + \lambda + \alpha) + A[(\Delta - \beta)^2 + (\frac{1}{2}A + \lambda + \alpha)^2]}, \quad (6.5)$$

which is independent of λ' . Furthermore, we note that the factor $\pi^{-1} \text{Re}[\dots]$ in Eq. (6.4) has strength of unity.

Equation (6.4) tracks down explicitly the dependence of $I_A(\omega)$ on the various mechanisms. Due to the presence of collisions, the resonance condition reads $\omega_L = \omega_0 + \beta$, since β is the collisional shift, and it is easy to check from Eq. (6.4) that on resonance ($\Delta - \beta = 0$) the spectrum is symmetric around $\omega = \omega_L$. The dependence on the second parameter λ' is illustrated in Fig. 3.

VII. MULTIMODE

From Eq. (2.17) for the probability distribution $P_\tau(x_2 | x_1)$, it follows that the jump process $x(t)$ has a finite memory time γ^{-1} . This prohibits the factorization of the average $\langle C(t', t) \rangle_{st}$ into a regression operator for the evolution $t \rightarrow t'$, acting on the average initial value $\langle C(t, t) \rangle_{st}$, as is the case for the diffusive phase [Eq. (6.1)]. Moreover, the average $\langle C(t, t) \rangle_{st}$ does not provide sufficient information for the evolution to $t' \geq t$, but $\langle C(t', t) \rangle_{st}$ depends also on the evolution of $C(t', t)$ in the recent past $t' < t$. Since the time evolution of $C(t, t)$ is determined by the equation of motion for $\sigma(t)$ [see Eq. (5.9)], the average $\langle C(t', t) \rangle_{st}$ will depend on both the regression equation (5.8) and on the time-evolution equation (3.11) for the atomic density operator. This problem of the so-called initial correlations of two-time averages has

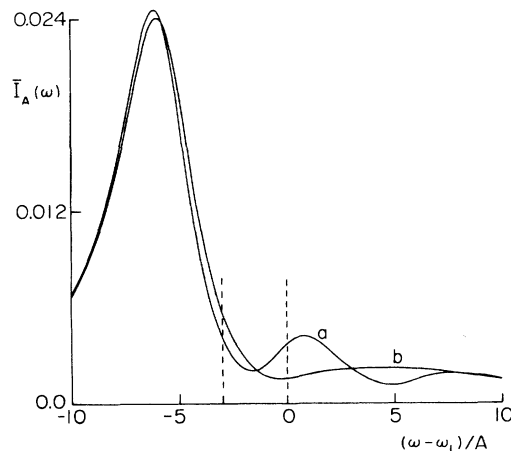


FIG. 3. The dimensionless absorption profile $\bar{I}_A(\omega) = I_A(\omega)A/BI_p$ as a function of the probe frequency. In curve *a* (*b*) we have taken $\lambda' = \lambda$ (4λ), and it is seen that for the Gaussian diffusion process (*b*), the line structure in the right (blue) wing is almost washed out, in comparison with the random-jump process (*a*). The dotted lines indicate the position of the laser frequency ω_L and the resonance $\omega_0 + \beta$. The shift of the absorption line to the left, with respect to the atomic resonance, is identified as the ac-Stark shift, which is due to the high intensity $\Omega^2 = 25A^2$. The other parameters are $\alpha = 1.5A$, $\lambda = A$, and $\Delta - \beta = 3A$.

been dealt with in detail in a previous paper,⁴² so here we merely apply the results.

If we solve the set of equations (3.11) and (5.8), which are tied together with the boundary condition (5.9), take the Fourier-Laplace transform, and substitute the result into Eq. (5.11), we obtain

$$I_A(\omega) = BI_p \frac{1}{\pi} \text{Re Tr} d^\dagger \frac{\gamma}{1 - \gamma \int dx P(x) U(\Lambda - x, x)} \times \int dx P(x) U(\Lambda - x, x) \{[d, U(0, x) \bar{\sigma}]\}, \quad (7.1)$$

for the absorption spectrum in the case of a multimode driving laser field. That we can express both resolvents in $U(\omega_1, \omega_2)$ is a consequence of the identity (4.11) and of the fact that the additional term in square brackets in Eq. (5.8), in comparison with Eq. (3.11), is just $x(t)$ times the unit operator. In general, averages like (7.1) require two different resolvents of the form $U(\omega_1, \omega_2)$. The absorption profile (7.1) is plotted in Fig. 4 for two different values of γ , but with all other parameters the same.

VIII. STRONG-FIELD LIMIT

In the absence of the driving laser ($\Omega^2 \rightarrow 0$) the atom is in the ground state ($n_g = 1$), and Eq. (6.4) reduces to

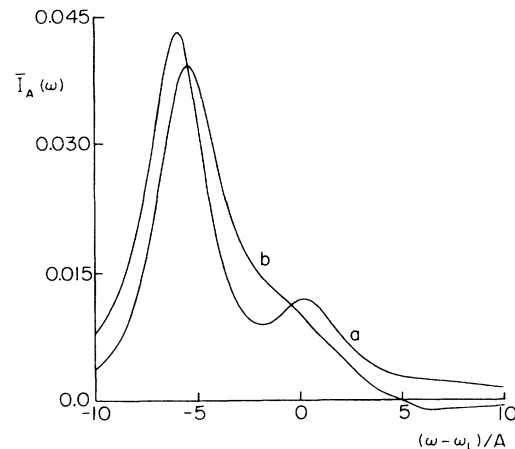


FIG. 4. The absorption profile from Eq. (6.1) for the same parameters as in Fig. 3, but with the single-mode laser replaced by a three-mode laser. The modes are situated at $\omega_L - 2A$, ω_L , and $\omega_L + 2A$ with relative probabilities of 1:2:1. The mode-switching rate equals $\gamma = 8A$ for curve *a* and $\gamma = 0.2A$ for curve *b*. We notice that curve *b* assumes negative values in the blue wing, which reflects an amplification of the probe beam, rather than a net absorption. Furthermore, we see that, in comparison with the single-mode case from Fig. 3, the absorption is roughly a factor of 2 larger for every ω . This is quite remarkable, since all optical and atomic parameters are the same. The only difference is the mechanism that brings about the laser width (phase fluctuations or mode switching).

$$I_A(\omega) = BI_p \frac{1}{\pi} \operatorname{Re} \frac{1}{\frac{1}{2}A + \alpha - i(\omega - \omega_0 - \beta)}, \quad (8.1)$$

which is a Lorentzian with a HWHM of $\frac{1}{2}A + \alpha$ at the resonance $\omega_0 + \beta$. The collisional width α adds to the natural width $\frac{1}{2}A$, and the line is shifted over β . This picture changes considerably for a strong incident field. Probing an atomic system by a laser amounts essentially to measuring the positions of the resonances and their widths, but for $\Omega^2 \neq 0$ these resonances are determined by the joint system of the atom and driving field, including their interaction, rather than by the atom itself, as is the case for $\Omega^2 = 0$. If we inspect Eq. (3.11) for the density operator $\sigma(t)$, we notice that the time evolution is determined by the Liouvillian $L_d(\omega_L)$, which represents the free evolution of the dressed atom. Phase fluctuations $[x(t)L_g]$, spontaneous decay $(-i\Gamma)$, and collisions $(-i\Phi)$ then affect the basic evolution, and give rise to relaxation of the system. Hence the positions of the resonances are fixed by the eigenvalues of $L_d(\omega_L)$, and their widths result from the details of the different damping mechanisms.

Diagonalizing the dressed-atom Hamiltonian H_d from Eq. (3.9) yields the eigenvalue equations for the dressed states $|\pm\rangle$,

$$H_d |\pm\rangle = \mp \frac{1}{2} \hbar \Omega' |\pm\rangle, \quad (8.2)$$

with

$$\Omega' = \Delta(1 + \Omega^2/\Delta^2)^{1/2}, \quad (8.3)$$

and the eigenvectors are found to be

$$|\pm\rangle = a_{\pm} |g\rangle \pm a_{\mp} |e\rangle. \quad (8.4)$$

The coefficients are given by

$$I_A(\omega) = BI_p \frac{A\Delta}{4(\frac{1}{2}A + \alpha + \lambda)\Omega} \left[\frac{1}{\pi} \operatorname{Re} \left[\frac{1}{\frac{1}{2}(3A/2 + \alpha + \lambda + \lambda') - i(\omega - \omega_L + \Omega)} \right] - \frac{1}{\pi} \operatorname{Re} \left[\frac{1}{\frac{1}{2}(3A/2 + \alpha + \lambda + \lambda') - i(\omega - \omega_L - \Omega)} \right] \right]. \quad (8.9)$$

The spectrum consists of two distinct Lorentzians, situated at $\omega = \omega_L \pm \Omega$, both with a HWHM of $\frac{1}{2}(3A/2 + \alpha + \lambda + \lambda')$, and both with equal strength. However, the line at $\omega_L + \Omega$ has an opposite sign, and corresponds to effective amplification. At the resonance ω_L , the line vanishes due to an exact cancellation of stimulated absorption and emission. Integration of Eq. (8.9) gives

$$\int d\omega I_A(\omega) = 0, \quad (8.10)$$

which can be understood from the fact that $n_e = n_g = \frac{1}{2}$ in the saturation limit. Comparison with Eq. (8.1) shows the peculiar feature that the collisional contribution to the linewidths is a factor of 2 less than in the low-intensity limit, and also the radiative width is altered. Further-

$$a_{\pm}^2 = \frac{1}{2}(1 \mp \Delta/\Omega'), \quad (8.5)$$

with the sign convention

$$a_- > 0, \quad a_+/\Delta > 0. \quad (8.6)$$

The dressed states of Liouville space then diagonalize $L_d(\omega_L)$ according to

$$L_d(\omega_L) |\pm\rangle \langle \pm| = 0, \quad (8.7)$$

$$L_d(\omega_L) |\pm\rangle \langle \mp| = \mp \Omega' |\pm\rangle \langle \mp|, \quad (8.8)$$

and therefore the resonances with respect to ω_L are situated at $\omega - \omega_L = 0$ (twofold degenerate) and $\omega - \omega_L = \mp \Omega'$. That the eigenvalues are shifted over the laser frequency ω_L is a result of the factor $\exp(-i\omega_L t)$ in the transformation (3.7).

The structure of the absorption spectrum can now be exhibited clearly in the secular approximation,⁹ which neglects the coupling between eigenvectors of $L_d(\omega_L)$ with different eigenvalues. In other words, we assume that each spectral line evolves independently. In view of Eq. (4.11), this should be imposed for every (effective) mode $\omega_L + x(t)$ separately in the multimode case. In this section we shall consider single-mode excitation, for which we have only the frequency ω_L . Then the linewidth gives rise to relaxation [the operators W_0 and W_+ in Eqs. (4.6) and (6.1), respectively], but not to additional resonances. The lines are positioned at $\omega_L - \Omega'$, ω_L , and $\omega_L + \Omega'$. Let us consider the situation of a strong laser field. Then the line separation $|\Omega'|$ equals Ω , and is brought about by the field intensity only. This is the ac-Stark shift. If we now evaluate the absorption profile (6.3) in the secular approximation and take the limit of large Ω , we find, for $\Delta > 0$,

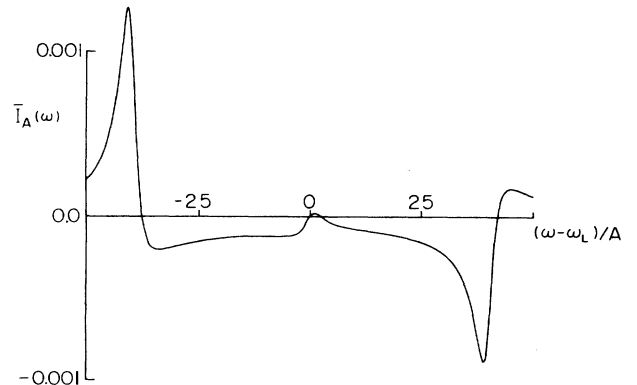


FIG. 5. Probe-absorption profile from Eq. (6.4) with parameters $\Omega = 40A$, $\Delta - \beta = 3A$, $\lambda = \lambda' = A$, and $\alpha = 1.5A$. The positions of the lines are determined by the laser intensity Ω^2 only.

more, we notice that the widths are proportional to the laser parameters λ' , but that the strengths depend only on λ . This property might supply an experimentally feasible method for the measurement of λ' . An example of a high-intensity profile is plotted in Fig. 5.

IX. CONCLUSIONS

We have studied the probe-absorption spectrum of a two-level atom in a nonmonochromatic laser field and a perturber bath. General, recently published theories on stochastic differential equations have been applied to obtain exact closed-form solutions for the average of the two-time dipole-correlation function in the steady state. This has been accomplished for both a single-mode field (independent-increment process for the phase) and a multimode laser (random-jump process for the time derivative of the phase). For single-mode irradiation the absorption profile appears to depend on the two laser parameters λ and λ' , where λ equals the linewidth, and λ' depends on the second-order intensity correlation. The parameter λ' ranges from $\lambda'=\lambda$ up to $\lambda'=4\lambda$ in general, and these two extreme limits give identical results as the Lorentz wave

(phase-jumping laser) and the phase-diffusion model [$\phi(t)$ is Gaussian white noise], respectively. The single-mode laser profile is a Lorentzian, but with the multimode representation we can model any laser line shape. A special case is the two-mode laser [random-telegraph signal for $x(t)$], which can also be solved with a more simple formalism.⁴² The tendency of the absorption spectrum to smoothen with increasing λ' or decreasing γ (mode-switching rate) is illustrated, and we find in Fig. 4 that even the sign of the net absorption could be changed by diminishing γ . This implies that an absorbing system becomes emissive if the laser switches faster between its modes, which is quite remarkable. Finally, we have elaborated on the high-intensity limit, for which the absorption profile appears to be antisymmetric with respect to the laser frequency.

ACKNOWLEDGMENTS

This research was supported by the National Science Foundation under Grant No. CHE-8519053 and the U.S. Air Force Office of Scientific Research under Contract No. F49620-86-C-0009.

-
- ¹B. R. Mollow, Phys. Rev. **188**, 1969 (1969).
²H. J. Carmichael and D. F. Walls, J. Phys. B **9**, 1199 (1976).
³H. J. Kimble and L. Mandel, Phys. Rev. A **13**, 2123 (1976).
⁴P. L. Knight and P. W. Milonni, Phys. Rep. **66**, 23 (1980).
⁵C. Cohen-Tannoudji, in *Frontiers in Laser Spectroscopy*, proceedings of the 27th Les Houches Summer School, edited by R. Balian, S. Haroche, and S. Liberman (North-Holland, Amsterdam, 1977), pp. 3ff.
⁶F. Schuda, C. R. Stroud, Jr., and M. Hercher, J. Phys. B **7**, L198 (1974).
⁷F. Y. Wu, R. E. Grove, and S. Ezekiel, Phys. Rev. Lett. **35**, 1426 (1975).
⁸B. R. Mollow, Phys. Rev. A **5**, 2217 (1972).
⁹C. Cohen-Tannoudji and S. Reynaud, J. Phys. B **10**, 345 (1977).
¹⁰F. Y. Wu, S. Ezekiel, M. Ducloy, and B. R. Mollow, Phys. Rev. Lett. **38**, 1077 (1977).
¹¹G. Nienhuis, J. Phys. B **14**, 1963 (1981).
¹²G. S. Agarwal, Phys. Rev. A **18**, 1490 (1978).
¹³H. F. Arnoldus and G. Nienhuis, J. Phys. B **16**, 2325 (1983).
¹⁴A. Omont, J. Phys. (Paris) **26**, 26 (1965).
¹⁵G. Nienhuis, J. Phys. B **15**, 535 (1982).
¹⁶K. Burnett, J. Cooper, P. D. Kleiber, and A. Ben-Reuven, Phys. Rev. A **25**, 1345 (1982).
¹⁷S. N. Dixit, P. Zoller, and P. Lambropoulos, Phys. Rev. A **21**, 1289 (1980).
¹⁸J. J. Yeh and J. H. Eberly, Phys. Rev. A **24**, 888 (1981).
¹⁹P. Zoller, G. Alber, and R. Salvador, Phys. Rev. A **24**, 398 (1981).
²⁰R. I. Jackson and S. Swain, J. Phys. B **15**, 4375 (1982).
²¹J. H. Eberly and K. Wódkiewicz, J. Opt. Soc. Am. **67**, 1252 (1977).
²²M. Kuš, Opt. Acta **31**, 261 (1984).
²³H. F. Arnoldus and G. Nienhuis, Opt. Commun. **54**, 95 (1985).
²⁴H. W. Lee, P. L. DeVries, I. H. Zimmerman, and T. F. George, Mol. Phys. **36**, 1693 (1978).
²⁵N. G. van Kampen, *Stochastic Processes in Physics and Chemistry* (North-Holland, Amsterdam, 1981).
²⁶J. L. Doob, *Stochastic Processes* (Wiley, New York, 1953).
²⁷J. H. Eberly, K. Wódkiewicz, and B. W. Shore, Phys. Rev. A **30**, 2381 (1984).
²⁸Z. Deng and J. H. Eberly, Opt. Commun. **51**, 189 (1984).
²⁹P. W. Anderson, J. Phys. Soc. Jpn. **9**, 316 (1954).
³⁰R. Kubo, J. Phys. Soc. Jpn. **9**, 935 (1954).
³¹H. F. Arnoldus and G. Nienhuis, J. Phys. B **19**, 873 (1986).
³²K. Wódkiewicz, B. W. Shore, and J. H. Eberly, Phys. Rev. A **30**, 2390 (1984).
³³H. F. Arnoldus and G. Nienhuis, J. Phys. B **19**, 2421 (1986).
³⁴W. H. Louisell, *Quantum Statistical Properties of Radiation* (Wiley, New York, 1973).
³⁵G. Nienhuis, Acta Phys. Pol. A **61**, 235 (1982).
³⁶P. Zoller, J. Phys. B **10**, L321 (1977).
³⁷A. T. George and S. N. Dixit, Phys. Rev. A **23**, 2580 (1981).
³⁸H. F. Arnoldus and G. Nienhuis, Opt. Acta **30**, 1573 (1983).
³⁹A. Brissaud and U. Frisch, J. Quant. Spectrosc. Radiat. Trans. **11**, 1767 (1971).
⁴⁰A. Brissaud and U. Frisch, J. Math. Phys. **15**, 524 (1974).
⁴¹V. E. Shapiro and V. M. Loginov, Physica **91A**, 563 (1978).
⁴²H. F. Arnoldus and G. Nienhuis, J. Phys. A **19**, 1629 (1986).
⁴³G. Nienhuis, Physica (Utrecht) **66**, 245 (1973).